Published December 15, 1996

Membrane Topology of the High-affinity L-Glutamate Transporter (GLAST-1) of the Central Nervous System

Stephan Wahle and Wilhelm Stoffel

Institute of Biochemistry I, Medical Faculty, University of Cologne, D-50931 Cologne, Germany

Abstract. The membrane topology of the high affinity, Na^+-coupled L-glutamate/L-aspartate transporter (GLAST-1) of the central nervous system has been determined. Truncated GLAST-1 cDNA constructs encoding protein fragments with an increasing number of hydrophobic regions were fused to a cDNA encoding a reporter peptide with two *N*-glycosylation sites. The respective cRNA chimeras were translated in vitro and in vivo in *Xenopus* oocytes. Posttranslational *N*-glycosylation of the two reporter consensus sites monitors the number, size, and orientation of membrane-spanning domains. The results of our experiments suggest a novel 10–transmembrane domain topology of GLAST-1, a representative of the L-glutamate neurotransmitter transporter family, with its NH_2 and COOH termini on the cytoplasmic side, six NH_2-terminal hydrophobic transmembrane α-helices, and four COOH-terminal short hydrophobic domains spanning the bilayer predicted as β-sheets.

L-Glutamate transporters are integral membrane glycoproteins. They are concentrated in the plasma membrane of glial cells and in nerve terminals surrounding the synaptic cleft, where they regulate the concentration of the excitatory neurotransmitter L-glutamate in the cleft of excitatory synapses (Flott and Seifert, 1991).

Two different families of neurotransmitter transporters have been identified. The Na^+-/Cl^--coupled GAT-1 transporter family includes the γ-aminobutyrate transporter (Guastella et al., 1990), the noradrenaline (Pacholczyk et al., 1991), dopamine (Shimada, et al 1991), serotonin (Blakely et al., 1991), glycine (Smith et al., 1992), and L-proline transporters (Fremeau et al., 1992). They share a 12-membrane–spanning domain topology (Uhl, 1992) with the carriers of the Na^+-dependent glucose transporter (SGLT-1) family (Hediger et al., 1987).

The recently discovered Na^+-dependent L-glutamate transporter GLAST-1[1] (Storck et al., 1992), GLT-1 (Pines et al., 1992), EAAC-1 (Kanai and Hediger, 1992), and EAAT-4, a Na^+/Cl^--dependent member isolated by homology screening (Fairman et al., 1995), form a second family of excitatory neurotransmitter transporters in the central nervous system. They catalyze an electrogenic cotransport of L-glutamate and two or three Na^+ ions coupled to the counterflow of one K^+ and probably one OH^- ion (Bouvier et al., 1992; Klöckner et al., 1993, 1994; Kanai et al., 1995). The members of this family show an overall amino acid identity of about 50%. The L-glutamate transporters are neither related to the GAT-1 nor to the SGLT-1 transporter family but show significant similarities (27–37%) to the neutral amino acid transporter ASCT-1 (Arizza et al., 1993) or SAAT (Shafqat et al., 1993), to the proton-coupled L-glutamate transporter proteins GLTP of *Escherichia coli* (Tolner et al., 1992*b*) and GLTT of *Bacillus stearothermophilus* (Tolner et al., 1992*a*), and to the C4-dicarboxylate carrier DCTA of *Rhizobium meliloti* (Engelke et al., 1989).

Three different transmembrane topology models of GLAST-1 (Storck et al., 1992), GLT-1 (Pines et al., 1992), and EAAC-1 (Kanai and Hediger, 1992) have been proposed, although the hydropathy plots are almost identical. In the NH_2-terminal half, they have six hydrophobic membrane-spanning α-helices and an extended extracellular loop (extramembrane region 4 [EMR4]) between transmembrane domain 3 (TMD3) and 4 (TMD4) with two *N*-glycosylation sites in common. For GLAST-1, we have shown by peptide sequencing (Schulte and Stoffel, 1995) and site-directed mutagenesis (Conradt et al., 1995) that two out of three putative *N*-glycosylation sites at N206 and N216 are glycosylated. The membrane topology of the highly conserved COOH-terminal domain of about 150 residues has been discussed controversially on the basis of their ambiguous hydropathy plot.

Pivotal for understanding the structure–function relationship and the regulation of the L-glutamate transporter

Address all correspondence to Wilhelm Stoffel, Joseph-Stelzmann-Str. 52, D-50931 Cologne, Germany. Tel.: 49-221-478-6881. Fax: 49-221-478-6882. E-mail: Wilhelm.Stoffel@rs1.rrz.uni-koeln.de

1. *Abbreviations used in this paper*: EAAC, excitatory amino acid carrier; EAAT, excitatory amino acid transporter; Endo F, endoglycosidase F; EMR, extramembrane region; GLAST, L-glutamate/L-aspartate transporter; GLT, glutamate transporter; RT, room temperature; TMD, transmembrane domain; VSV, vesicular stomatitis virus G protein.

Published December 15, 1996

is the comprehensive knowledge of the membrane topology of these important transporters of excitatory neurotransmitters in the central nervous system. In the present study, we investigated the glutamate transporter topology by the "reporter glycosylation scanning" strategy. This direct biochemical method, which has been used successfully for topological mapping of polytopic KDEL-receptor (Singh et al., 1993), analyzes the glycosylation sensitivity of a topological neutral reporter epitope placed in positions to bracket the proposed transmembrane domains. This approach was complemented by the determination of the use of N-linked glycosylation sites introduced in the wild-type transporter and by immunofluorescent studies.

Our results with the GLAST-1 glutamate transporter demonstrate six membrane-spanning domains of most likely α-helical structure (TMD 1–6) in the NH_2-terminal part of the protein and four shorter transmembrane segments (TMD 7–10) in the COOH-terminal part of the protein, with both termini residing on the cytoplasmic surface of the plasma membrane. We suggest that this novel 10-TMD topology might be common to the other members of the L-glutamate transporter family.

Materials and Methods

Construction of Undeleted and Deleted Fusion Proteins

The plasmid pSP64-GLAST (Storck et al., 1992) served as template in the creation of the fusion proteins. The AccI site in the multiple cloning site of pSP64-GLAST was eliminated by a SalI digestion, filling in reaction with Klenow enzyme and blunt-end religation with T4 ligase (Boehringer Mannheim Corp., Indianapolis, IN). The DNA fragment coding for the glycosylation reporter (D172-R228 of GLAST-1) was amplified in a PCR carrying in frame at the 5′-end a SacI and XhoI and at the 3′-end a TAG stop codon and SacI restriction site. The reporter fragment was cloned into the SacI site downstream of the GLAST-1 gene in pSP64-GLAST resulting in pSP64-GLAST-REP. Fusions of transporter fragments to the glycosylation reporter segment were achieved by replacing COOH-terminal domains of the full-length GLAST-1 cDNA in pSP64-GLAST-REP between a suitable 5′ restriction site and the XhoI site 3′ in front of the glycosylation reporter with PCR-generated DNA cassettes, coding for respective COOH-terminal parts of graded NH_2-terminal stretches of the transporter. A NheI 5′ restriction site in the GLAST-1 gene was used for fusion proteins G-E77, G-R122, and G-P233; KpnI was used for G-S273, G-Q313, G-N344, G-Q354, and G-T368; AccI was used for G-R385, G-E406, G-Q425, G-T434, and G-Q445; and HincII was used for G-D464, G-D487, G-E501, G-I514, and G-M543 (see Fig. 1 *B*).

The deletion of putative COOH-terminal transmembrane domains was introduced into the fusion proteins by overlapping extension PCR (Higuchi et al., 1988). Amplified fragments containing the desired deletions corresponding to GLAST-1 amino acid residues 345–354, 389–397, 407–416, and 488–494 were digested with AccI and XhoI present in the undeleted fusion protein sequences to obtain DNA cassettes, which were exchanged for the respective wild-type cassettes of G-R385, G-E406, G-Q425, G-E501, and G-M543. This resulted in the cDNA chimeras coding for ΔG-R385 (Δ345–354), ΔG-E406 (Δ389–397), ΔG-Q425 (Δ407–416), ΔG-E501 (Δ488–494), and ΔG-M543 (Δ488–494) (see Fig. 1 *C*). All constructs were characterized by restriction enzyme analysis and DNA sequencing.

Insertion of Glycosylation Sites and Single Substitutions

Unique *N*-glycosylation sites (consensus sequence N/X/T or N/X/S; Hart et al., 1978) were introduced into the GLAST-1 gene of pSP64-GLAST at position 1143 and 1303 by overlapping extension PCR. The replacement of the sequences GTG and GCC by ACG and AAC led to the single–amino acid substitutions T382V and N435A. The PCR fragments containing the desired mutations were cut with KpnI and HincII and inserted into the GLAST-1 gene, replacing the respective wild-type cassette. The mutant transporters G-T382V and G-N435A were obtained.

The mutant transporters G-EL389FV, G-T382V/EL389FV, and G-T382V/VSV were constructed by site-directed mutagenesis. An XhoI site was introduced into wild-type GLAST-1 and the mutant transporter G-T382V by the same strategy as for the insertion of *N*-glycosylation sites. The replacement of TTTGTG by CTCGAG at position 1164 corresponds to the amino acid substitutions E389F and L390V and resulted in cDNAs of G-EL389FV and G-T382V/EL389FV. Sense and antisense oligonucleotides encoding the COOH terminus (YTDIEMNRLGK) of the vesicular stomatitis virus G protein (VSV) (Kreis, 1986) were synthesized to insert an extension peptide at the COOH terminus of residue L390 in G-T382V/EL389FV. The annealed double-stranded oligonucleotides flanked by sticky-ended XhoI sites were phosphorylated with T4-polynucleotide kinase (Boehringer Mannheim Corp.) and cloned into the engineered XhoI site, resulting in G-T382V/VSV. All mutations and subcloned nucleotide sequences were verified by DNA sequencing.

RNA Transcription

Plasmids were linearized with EcoRI. The respective methyl-diguanosine-triphosphate–capped cRNAs were synthesized from their corresponding linearized templates using SP6 RNA polymerase (Boehringer Mannheim Corp.) following standard methods (Colman, 1984). RNA quality was checked by electrophoresis in formaldehyde (1.2%) agarose gel.

Cell-free Translation and Deglycosylation

In vitro synthesized cRNA (300–500 ng) was translated in micrococcal nuclease–treated rabbit reticulocyte lysate (amino acid depleted; Amersham Corp., Arlington Heights, IL) in the presence of canine pancreatic rough microsomal membranes (Boehringer Mannheim Corp.) according to the supplier's instructions. The reaction mixture (25 μl total volume) with optimal translation efficiency contained 1,110 kBq [^{35}S]methionine (Amersham Corp.), 25 μM of each amino acid except methionine, 100 mM potassium acetate, and 2 mM magnesium acetate and was incubated at 30°C for 60 min.

After addition of 25 μl STPM (0.25 M sucrose, 50 mM triethanolamine, 140 mM potassium acetate, and 2.5 mM magnesium acetate) membranes were pelleted by ultracentrifugation for 10 min and rinsed with 50 μl STPM. One aliquot was resuspended in 50 μl Laemmli sample buffer (62.5 mM Tris-HCl, pH 6.8, 10% glycerol, 5% mercaptoethanol, 1% SDS, and 0.04% bromophenol blue) and the other in 25 μl 0.75% Triton X-100, 30 mM Tris-HCl, pH 8, for deglycosylation with endoglycosidase F (Endo F; 50 mU) (Boehringer Mannheim Corp.) for 1 h at 37°C. The reaction was terminated by the addition of 25 μl 2× Laemmli sample buffer. Proteins were analyzed by SDS-PAGE (Laemmli, 1970) followed by fluorography (Laskey and Mills, 1975).

Alkaline Extraction

The pH of the in vitro translation assay, carried out in the presence of rough microsomal membranes, was adjusted to 11.5 by the addition of 25 μl of carbonate buffer (50 mM potassium acetate, 100 mM Na_2CO_3, 20 mM triethanolamine, and 1 mM magnesium acetate). The reaction mixture was stored on ice for 20 min and layered over 20 μl STPM containing 100 mM Na_2CO_3. Microsomes were sedimented at 49,000 rpm at 4°C for 20 min. The pellet was washed with 25 μl STPM and dissolved in 30 μl Laemmli sample buffer. The supernatant was neutralized with 10 μl acetic acid and proteins were precipitated with two volumes of saturated ammonium sulfate for 30 min at 0°C, sedimented at 14,000 rpm, 4°C for 10 min. The pellet was washed with 5% trichloroacetic acid and dissolved in 50 μl Laemmli sample buffer for SDS-PAGE.

Expression in Oocytes, Immunoprecipitations, and Glycosidase Treatment

Stage V–VI oocytes were defolliculated with collagenase and injected with 40 nl of cRNA of mutant GLAST-1 construct (0.5 mg/ml) (Storck et al., 1992). Oocytes were incubated in Barth's modified saline containing [^{35}S]methionine (2.5 mCi/ml) for 24 h. Deglycosylation with Endo F and immunoprecipitation with polyclonal GLAST-1 antibody was performed as previously described (Conradt et al., 1995). Translation products were analyzed by SDS-PAGE (Laemmli, 1970) followed by fluorography (Laskey and Mills, 1975).

Published December 15, 1996

Electrophysiology

Electrogenic transport was assayed by voltage clamp using the two electrode voltage clamp amplifier (Warner Instruments Corp., Hamden, CT; hardware and software package ISO2 from MFK, Frankfurt, Germany). Briefly, oocytes were voltage clamped at −90 mV and continuously superfused with Barth's modified saline. Microelectrodes filled with 3 M KCl had a resistance ranging from 1–2 MΩ.

Immunofluorescence Microscopy

Preparation of oocyte frozen thin sections and immunofluorescence microscopy on the fusion proteins and mutant transporters were carried out as described previously (Conradt and Stoffel, 1995).

For immunofluorescence on HEK293 cells, permanently expressing GLAST-1 (Blau and Stoffel, 1995) cells were grown on coverslips, rinsed with PBS, fixed with 2% paraformaldehyde in PBS for 15 min at room temperature (RT), permeabilized with 0.25% Triton X-100 in PBS for 5 min at RT, blocked with 5% BSA in PBS for 1 h at RT, incubated with primary antibodies in PBS containing 2% BSA for 3 h at RT, incubated with secondary antibody in PBS containing 2% BSA, and then mounted with use of glycerol gelatine (Merck, Darmstadt, Germany).

The primary antibodies were affinity-purified rabbit anti–GLAST-1 antibody (Storck et al., 1992), monoclonal mouse anti–α-tubulin antibody (Sigma Chemical Co., St. Louis, MO), and polyclonal rabbit anti–P24-40 antibody. Secondary antibodies were FITC-conjugated goat anti–rabbit/anti–mouse IgG and Cy3-conjugated sheep anti–rabbit IgG (Sigma Chemical Co.).

Stained cells and frozen thin sections of oocytes were visualized with a fluorescence microscope (Axiophot; Carl Zeiss, Inc., Thornwood, NY) equipped with fluorescein and Cy3 optics and photographed with a microscope camera (model MC 100; Carl Zeiss, Inc.).

Polyclonal Antipeptide Antibody

The synthetic peptide corresponding to the NH_2-terminal residues 24–40 of rat GLAST-1 protein (KRTLLAKKKVQNITKED) was synthesized on a peptide synthesizer (model 433A; Applied Biosystems, Inc., Foster City, CA) following the manufacturer's instructions. The peptide was characterized by reversed phase high performance liquid chromatography and sequencing. It was coupled to keyhole limpet hemocyanin (Sigma Chemical Co.) (Goodfriend et al., 1964). 400 μl protein–peptide conjugate in PBS (300 μg peptide) was emulsified with an equal volume of complete Freund's adjuvant and injected intramuscularly in a New Zealand White rabbit. For booster immunizations (2-wk intervals), Freund's incomplete adjuvant and half the amount of antigen were used. The rabbit was bled 10 wk after the first immunization.

The antibody was characterized against a purified preparation of GLAST-1 protein (Western blot) and chimeric protein G-E77 by immunoprecipitation. For affinity purification (Catty, 1988), the synthetic peptide was coupled to ethylaminohexyl Sepharose 4B (Pharmacia LKB Biotechnology, Piscataway, NJ). Ethylaminohexyl–Sepharose (30 μmol active amino groups) was incubated with 10 mg peptide and 90 μmol *N*-ethoxycarbonyl-2-ethoxy-1,2-dihydroquinoline (Sigma Chemical Co.) in 6 ml 50% ethanol overnight at RT. The column material was rinsed three times with 50, 100, 50, and 20% ethanol, blocked with 0.2 M glycine, pH 8, for 2 h at RT and washed with PBS. 10 ml antiserum was recircled over the affinity column for 2 h. Unspecific bounded proteins were disrupted by washing with 10 mM Tris-HCl, pH 7.5, 0.5 M NaCl. Specific antibodies were eluted with 0.2 M glycine-HCl, pH 2.5, neutralized with 1 M Tris-HCl, pH 8, and dialyzed against PBS for 3 d.

Results

Chimeras with a Glycosylation Reporter Probe the Sidedness of Membrane Integration of GLAST-1

Our goal was to identify which of the hydrophobic protein segments actually span the membrane (TMDs) and to determine the cellular orientation of the membrane-flanking EMRs. We mapped the luminal or cytoplasmic orientation of the intervening hydrophilic loops with an endogenous reporter of translocation. It was fused in frame to

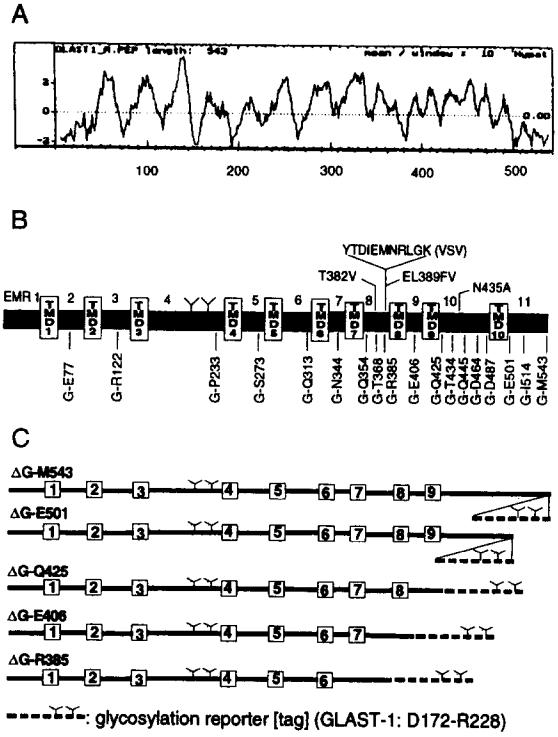

Figure 1. (*A*) Hydropathy plot of GLAST-1. The Kyte-Doolittle method with a window of 10 amino acids was applied. Six extended hydrophobic regions are located in the NH_2-terminal part of GLAST-1 (M1-P345) corresponding to the predicted transmembrane domains TMD1–TMD6. At least seven short, moderately hydrophobic segments are indicated in the COOH-terminal part. (*B*) Schematic model of the GLAST-1 transporter. Endogenous *N*-glycosylation sites are indicated by "trees." Boxes labeled with TMD denote topogenic hydrophobic regions as indicated by the present study. Identified hydrophilic EMRs are marked as EMR1–EMR11. The vertical lines below the solid heavy line indicate the COOH termini of NH_2-terminal GLAST-1 fragments, to which the glycosylation reporter was fused. The vertical lines above indicate the positions of substituted amino acids introduced either to generate additional *N*-glycosylation sites in the primary sequence (T382V, N435A) or to insert the VSV extension peptide of 11 amino acids into GLAST-1 (EL389FV). (*C*) Schematic presentation of GLAST-1 deletion chimeras. Membrane-spanning regions are numbered and marked by empty squares. A 57–amino acid *N*-glycosylation reporter derived from EMR4 of GLAST-1 was fused in frame to truncated GLAST-1 sequences. The deletion chimeras each lack the ultimate COOH-terminal transmembrane domain of the corresponding undeleted chimeras with identical fusion points.

NH_2-terminal parts of GLAST-1, truncating the transporter at various positions in the extramembrane regions (Fig. 1 *B*). This 57-residue *N*-glycosylation reporter was derived from the large extracellular hydrophilic loop of GLAST-1 (D172-R228), which contained the two genuine transporter *N*-glycosylation sites at N206 and N216 (Conradt et al., 1995; Schulte and Stoffel, 1995). This reporter sequence is considered to be devoid of any targeting information, which might interfere with its translocation across the membrane. The cRNAs of the chimeras were expressed in the presence of [^{35}S]methionine in vitro in reticulocyte lysates with rough microsomes and upon microinjection in *Xenopus* oocytes. The glycosylated

Published December 15, 1996

translation products were immunoprecipitated and analyzed by SDS-PAGE and fluorography. The orientation of the polypeptides integrated into the ER membrane is inverted from that in the plasma membrane. Bi-antennary *N*-glycosylation of the reporter sequence proved by the mobility shift in SDS-PAGE after digestion with Endo F characterized chimeras with the reporter protruding into the lumen of the ER. This corresponds to an extracellular orientation of the attached hydrophilic region in the plasma membrane; the absence of reporter glycosylation is indicative of its intracellular orientation.

Topology of the Six Hydrophobic Segments of the NH_2-Terminal Domain

The hydropathy plot of GLAST-1 (Fig. 1 *A*) clearly subdivides the protein into two large domains. In contrast to the extended moderately hydrophobic stretch (amino acids 345–500) near the COOH terminus of the transporter, the NH_2-terminal domain of nearly 345 amino acids has six distinct hydrophobic domains 20 to 23 residues in length (TMD1–TMD6 in Fig. 1 *B*), bordered by charged residues. They have been previously predicted to form transmembrane α-helices. They are connected by six hydrophilic extramembrane regions (EMR2–EMR7), to each of which the *N*-glycosylation reporter was fused at positions indicated in Fig. 1 *B*. Corresponding results were obtained in both expression systems. *N*-glycosylation was detected only of the reporters linked to residues E77, P233, and Q313. Chimera G-E77, truncating the transporter sequence at E77 in EMR2, yielded a bi-antennary glycosylated polypeptide as evidenced by the 6-kD mobility shift after Endo F treatment (Fig. 2 *A*, lane *1–4*). Fusion proteins G-P233 and G-Q313 tagging EMR4 and EMR6 (Fig. 2 *A*, lane *9–12*; Fig. 2 *B*, lane *5–8*) were fourfold glycosylated, twice at the reporter and at both genuine GLAST-1 glycosylation sites (N206 and N216). When digested with Endo F, protein size decreased for ~12 kD. On the other hand, *N*-glycosylation was not observed for reporters fused to EMR3, EMR5, or EMR7. The apparent molecular mass of chimera G-R122 (Fig. 2 *A*, lane *5–8*) remained unchanged after enzymatic deglycosylation. The predominant translation product of chimeras G-S273 (Fig. 2 *B*, lane *1–4*) and G-N344 (Fig. 2 *B*, lane *9–12*) exhibited only a 6-kD mobility shift and were thus only twofold glycosylated at genuine GLAST-1 consensus sites. In the case of in vitro–expressed G-S273, an insignificant amount of three- and fourfold glycosylated polypeptides is visible (both upper bands in Fig. 2 *B*, lane *1*). A phenomenon we observed for most of the in vitro translations performed in this study was the appearance of a signal representing unglycosylated and thus unprocessed protein. This is almost absent in the oocyte experiments. Furthermore, all six fusion proteins were found to be integrated into the lipid bilayer of microsomal membranes by the criterion of nonextractability with sodium carbonate at alkaline pH (Fujiki et al., 1982; Russel and Model, 1982) (data not shown).

We conclude from these results that the hydrophilic sequences EMR2, EMR4, and EMR6 are exposed to the extracellular, EMR3, EMR5, and EMR7 to the cytosolic surface of the plasma membrane. Each of the hydrophobic segments in the NH_2-terminal part of GLAST-1 is sandwiched between an extracellular and intracellular region indicating six TMDs. TMD1, TMD3, and TMD5 span the plasma membrane from the intracellular to the extracellular surface, and TMD2, TMD4, and TMD6 span with reverse orientation.

Membrane Topology of the Conserved COOH-Terminal Domain of GLAST-1

Previous models of three L-glutamate transporters have proposed two (GLT-1), four (EAAC-1), or six (GLAST-1) hydrophobic domains spanning the plasma membrane in the highly conserved COOH-terminal domain, albeit the hydropathy blot is too ambiguous for a reliable structure prediction. 12 additional reporter chimeras step-wise extended the NH_2-terminal domain of GLAST-1 by 10–29

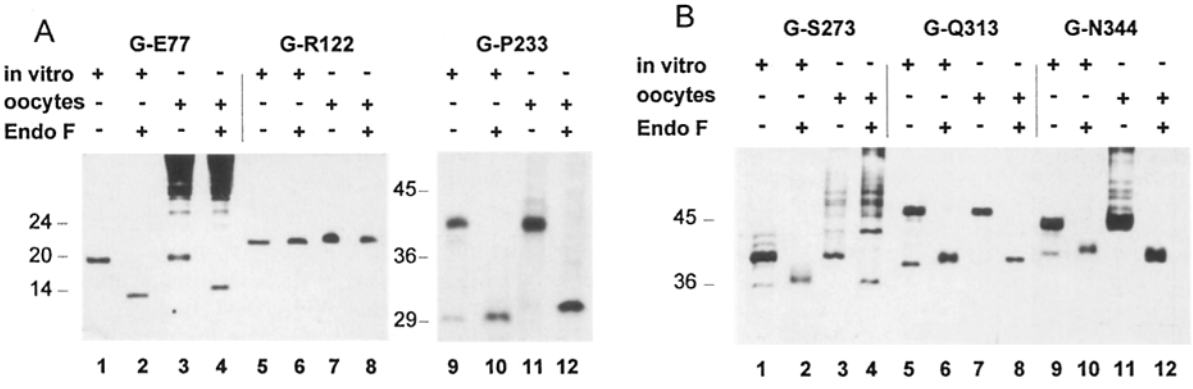

Figure 2. Analysis of the topology of the NH_2-terminal part of GLAST-1. *N*-glycosylation and membrane integration of chimeras with the reporter fused at sites located within the NH_2-terminal domain of GLAST-1: (*A* and *B*) GLAST-1 reporter hybrids were translated in the rabbit reticulocyte lysate system in the presence of microsomal membranes and upon microinjection in *Xenopus* oocytes. Translation products were isolated by ultracentrifugation of the microsomal membranes (in vitro) or by immunoprecipitation with a polyclonal GLAST-1 antibody from the oocyte lysate in the in vivo experiment. Proteins were separated by SDS-PAGE (10–15%) and visualized by fluorography (see Materials and Methods). Concordant results were obtained in both expression systems used. Treatment with Endo F reduced the apparent molecular mass of chimeras G-P233 and G-Q313 by ~12 kD, and of G-E77, G-S273, and G-N344 by ~6 kD. No mobility shift was observed in the case of G-R122.

Published December 15, 1996

amino acids, starting at amino acid Q354 near the COOH terminus of TMD6 up to M543 (see Fig. 1 *B*). When translated in both expression systems, chimeras G-E406 (Fig. 3 *B*, lanes *1–4*), G-E501, G-I514, and G-M543 (Fig. 3 *D*, lanes *1–12*) exhibited only a 6-kD mobility shift after Endo F treatment monitoring nonmodified reporter sites. We conclude that the short hydrophilic region around residue E406 (EMR9 in Fig. 1 *B*) as well as the highly charged COOH terminus of GLAST-1 (residues E501–M543; EMR11 in Fig. 1 *B*) are exposed on the cytoplasmic side of the ER or plasma membrane.

Unexpectedly, in vitro and in vivo translation of chimeras G-Q354, G-T368, G-R385, (Fig. 3 *A*, lanes *1–12*), G-Q425, G-T434 (Fig. 3 *B*, lanes *5–12*), G-Q445, G-D464, and G-D487 (Fig. 3 *C*, lanes *1–12*) generated two differently glycosylated polypeptides of approximately equal intensity in autoradiography. Endo F reduced their apparent molecular mass by roughly 12 and 6 kD and resulted in a single band of deglycosylation product. The weak signals in the in vitro translations of G-T368 and G-R385 (Fig. 3 *A*, lanes *5* and *9*) represent trace amounts of one- and threefold glycosylated polypeptides. However, these results indicated that the reporter of nearly one half (40–55%) of each expressed chimeric protein was fully glycosylated, yielding a tetra-antennary glycoprotein with the COOH-terminal reporter protruding into the lumen of the ER (upper band in Fig. 3, *A* and *C*, lanes *1*, *3*, *5*, *7*, *9*, and *11*; Fig. 3 *B*, lanes *5*, *7*, *9*, and *11*). The reporter of the rest of the integrated polypeptides remained unglycosylated on the cytoplasmic side of the membrane represented by biantennary glycoprotein. Reflecting the random orientation of the reporter, this glycosylation pattern seemed to be devoid of any topological information. Nevertheless, we obtained evidence to indicate the lumenal localization of the tagged EMRs from the following experiment.

A third *N*-glycosylation signal at N380 (G-T382V) and N435 (G-N435A) was introduced in wild-type GLAST-1 using site-directed mutagenesis (see Fig. 1 *B*). Tri-antennary glycosylation would probe the lumenal/extracellular orientation of the new consensus sites in membrane-integrated GLAST-1. However, polypetides synthesized in *Xenopus* oocytes from G-T382V and G-N435A cRNAs had the same size as the wild-type transporter. Enzymatic deglycosylation reduced the molecular mass from 60–63 to 54–57 kD (Fig. 4, lanes *1–6*). *N*-glycosylation of the engineered consensus sites should fail if they are located in the cytosolic compartment or if their close proximity to the lumenal membrane surface prevents access for the *N*-glycosylation machinery. We favored the second possibility and extended the short distance between residue N380 and the

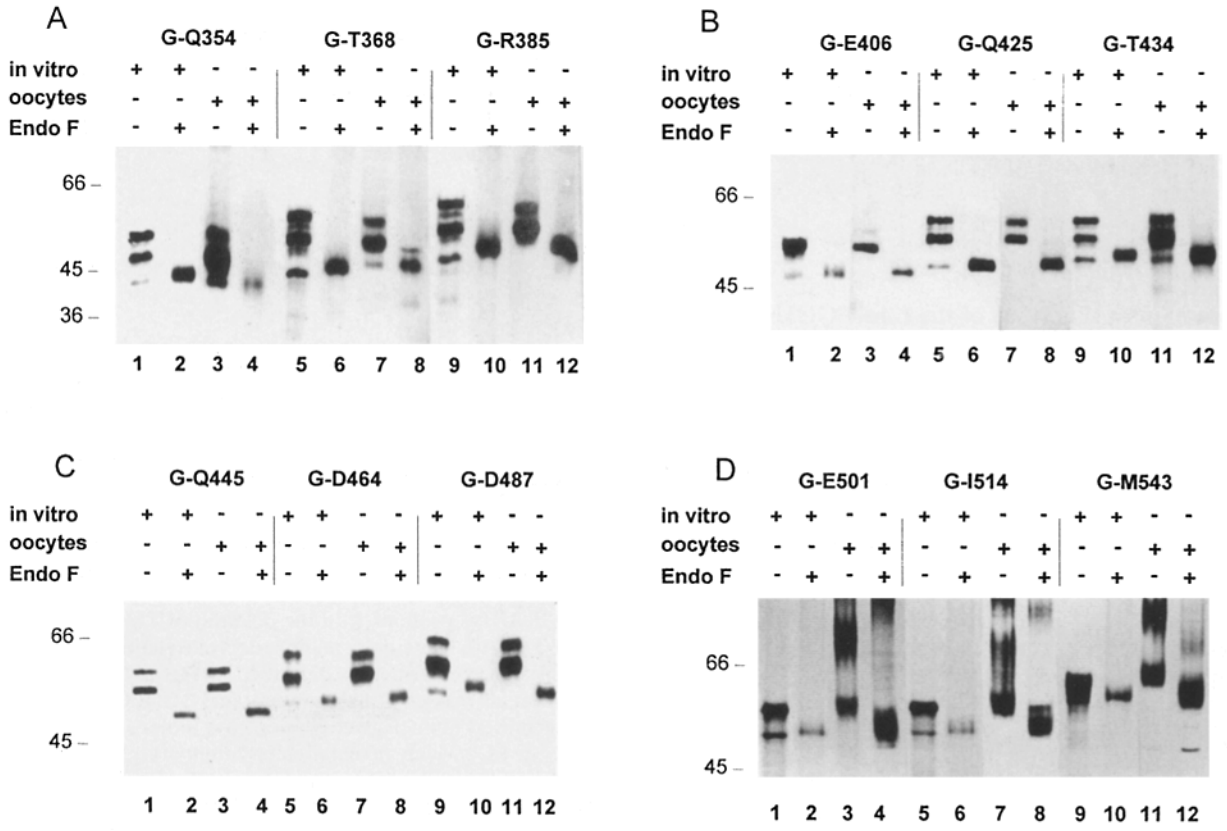

Figure 3. Analysis of the topology of the COOH-terminal part of GLAST-1. *N*-glycosylation and membrane integration of in vitro– and in vivo–translated chimeras with the reporter fused at sites located within the COOH-terminal domain of GLAST-1: (*A–D*) Protein expression, deglycosylation, and sample analysis was performed as described in Fig. 2. The chimeras G-E406, G-E501, G-I514, and G-M543 were twofold glycosylated as indicated by their reduced apparent molecular mass of ~6 kD after treatment with Endo F. Note that chimeras G-Q354, G-T368, G-R385, G-Q425, G-T434, G-Q445, G-D464, and G-D487 showed a random distribution of bi- and tetra-antennary glycosylated translation products, indicated by their apparent SDS-PAGE mobility shifts relative to the deglycosylated proteins of ~6 and 12 kD, respectively.

Published December 15, 1996

membrane surface by a short peptide consisting of the 11 COOH-terminal amino acids of the VSV glycoprotein (Kreis et al., 1986). The two-step cDNA synthesis (see Materials and Methods) yielded two different transporter mutants. The intermediate construct G-T382V/EL389FV carried the amino acid substitutions E389F and L390V, G-T382V/VSV in addition to the VSV extension peptide (see also Fig. 1 *B*). *Xenopus* oocytes microinjected with the respective cRNAs generated threefold glycosylated polypeptides (Fig. 4, lanes *7–10*). The apparent molecular mass of ~63–66 kD exceeded by ~3 kD that of the mutant G-EL389FV, which lacked the engineered *N*-glycosylation site at N380 (Fig. 4, lanes *11–12*), and was reduced to 54–56 kD by Endo F treatment. These findings provide strong evidence for the lumenal orientation of the hydrophilic region around residue N380 (EMR8 in Fig. 1 *B*). Because the fusion point of the chimera G-R385 was also located in this domain, we interpret its random bi- and tetra-antennary glycosylation in strong support of the extracellular orientation of respective reporter-attached residues located in the COOH-terminal domain of GLAST-1 (residues 345–543). We had observed the same glycosylation pattern for chimeras with the reporter linked to residues Q354, T368, and R385, as well as to Q425, T434, Q445, D464, and D487, and therefore suggest two additional extramembrane regions, EMR8 and EMR10, on the extracellular surface of the plasma membrane (Fig. 1 *B*). Keeping in mind the cytosolic placement of EMR7, EMR9, and EMR11, the alternating cytosolic and extracellular orientation of the five identified extramembrane regions EMR7–EMR11 demands four hydrophobic transmembrane domains (TMD7–TMD10) spanning the plasma membrane in the COOH-terminal part of GLAST-1.

Deletion of Transmembrane Segments in the COOH-terminal Domain of GLAST-1

The hydropathy plot (Fig. 1 *A*) of the four COOH-terminal TMDs identified by the experiments described above suggests short hydrophobic segments of 7–10 residues. To confirm their topogenic activity, we deleted each of these segments and examined the effect of this manipulation on the glycosylation reporter fused COOH-terminal to the respective TMD (Fig. 1 *C*). It is expected that an extracellular location of the fusion site of chimeras with the reporter linked to TMD7 and TMD9, being randomly two- and fourfold glycosylated, will switch to the intracellular surface in the deletion mutant, thus preventing reporter glycosylation. We synthesized the deletion chimeras ΔG-R385 (Δ P345–Q354) and ΔG-Q425 (Δ A407–V416) in the in vitro and in vivo system. The size of the single glycosylated translation product was reduced by 6 kD after Endo F treatment (Fig. 5 *A*, lanes *1–8*). This indicated that the reporter remained unglycosylated on the cytosolic side of the membrane. To show that deletion of TMD8 and TMD10 also changes the glycosylation pattern of the reporter fused COOH-terminal to these TMDs, we excised residues F389–I397 in chimera G-E406 and residues S488–V494 in G-E501 and G-M543 (Fig. 1 *C*). Unlike the unde-

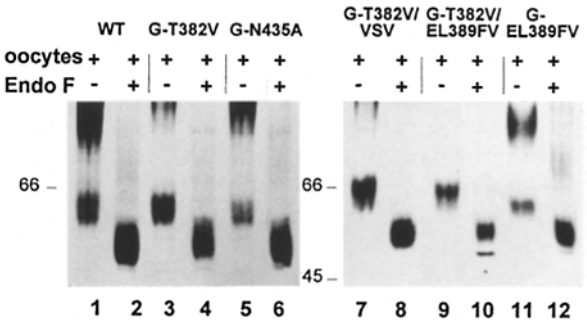

Figure 4. *N*-glycosylation of wild-type and mutant GLAST-1 proteins expressed in *Xenopus* oocytes. Protein expression, deglycosylation, immunoprecipitation, and sample analysis were carried out as described in Fig. 2. The equal SDS-PAGE mobility shifts of mutants G-T382V and G-N435A of ~6 kD after treatment with Endo F as compared with wild-type GLAST-1 indicated a twofold glycosylation of the proteins. The apparent molecular mass of constructs G-T382V/EL389FV and G-T382V/VSV exceeded that of G-EL389FV by ~3 kD, indicating threefold glycosylation of both mutants.

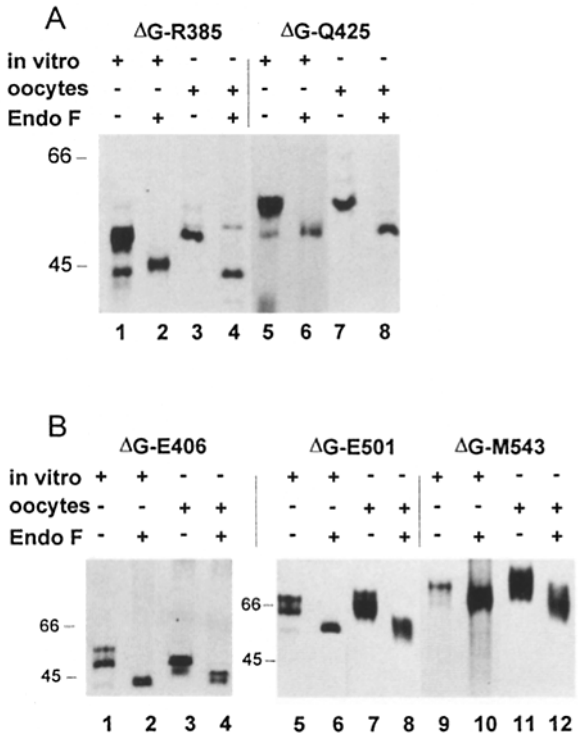

Figure 5. *N*-glycosylation of in vitro– and in vivo–synthesized chimeric GLAST-1 proteins with the deletion of TMD7, TMD8, TMD9, or TMD10. Protein expression, deglycosylation, and sample analysis were performed as described in Fig. 2. (*A*) The apparent molecular masses of deletion mutants ΔG-R385 and ΔG-Q425 were shifted after deglycosylation to a molecular mass reduced by ~6 kD, which revealed a bi-antennary glycosylation only compared to the respective undeleted GLAST-1 constructs with their random tetra- and bi-antennary glycosylation (see Fig. 3, *A* and *B*). (*B*) The reporter of ΔG-E501 is partially glycosylated in both expression systems as demonstrated by the two bands with different mobilities. The same observation was made for in vitro–synthesized ΔG-E406. Note that ΔG-E406 expressed in the oocyte, as well as ΔG-M543 in both expression systems, showed only one signal of a twofold glycosylated protein indicated by the 6-kD shift like in the undeleted chimeras (see Fig. 3). No glycosylation of the reporter sites had occurred.

Published December 15, 1996

leted fusion proteins, which are only twofold glycosylated, the deletion chimera ΔG-E406 translated in the reticulocyte lysate and ΔG-E501 regardless of the expression system used showed the expected random bi- and tetra-antennary glycosylation (Fig. 5 *B*, lanes *1* and *2* and *5–8*; compare Fig. 3 *B*, lanes *1* and *2*, and 3 *D*, lanes *1–4*). This glycosylation pattern indicates the extracellular orientation of the fusion points, which had switched from the intracellular to extracellular side. ΔG-E406 synthesized in the oocyte carried only two carbohydrate chains at endogenous N206 and N216, like the undeleted fusion protein (Fig. 5 *B*, lanes *3* and *4*; compare Fig. 3 *B*, lanes *3* and *4*). The upper band in lane *4* of Fig. 5 *B* reflects incomplete enzymatic deglycosylation. Unexpectedly, the deletion of TMD10 in the chimera G-M543 did not invert the cytosolic orientation of the fusion point (Fig. 5 *B*, lanes *9–12*; compare Fig. 3 *D*, lanes *9–12*). These results prove that the deleted hydrophobic segments P345–Q354, A407–V416, and S488–V494 are core sequences of the membrane-spanning domains TMD7, TMD9, and TMD10. The topogenic activity of TMD8 (F389–I397) could not be concluded with certainty from these experiments.

GLAST-1 Fusion Proteins Are Correctly Targeted to the Plasma Membrane but Inactive Transporters

The impact of the truncation and COOH-terminal tagging by a reporter sequence of GLAST-1 on the electrogenic, Na^+-dependent L-glutamate transport function was analyzed with the whole cell voltage clamp technique in *Xenopus* oocytes expressing the respective transporter cRNAs. The inward current of oocytes synthesizing the different chimeras was measured at 100 μM L-glutamate and 90 mM sodium [Na^+] extracellular concentrations as previously described (Klöckner et al., 1993). Neither wild-type GLAST-1 linked to the *N*-glycosylation reporter (G-M543) nor any of the other fusion proteins showed any neurotransmitter transport activity (data not shown). The loss of function could either be due to a reduced expression level, to a reduced stability of the mutant transporters, to an impaired targeting to the plasma membrane, or to the COOH-terminal truncation of GLAST-1 and tagging by the reporter sequence. Comparable intensities of the [^{35}S]methionine-labeled and immunoprecipitated translation products of GLAST-1 (Fig. 4, lanes *1* and *2*) and chimeric transporters (Figs. 2 and 3) expressed in *Xenopus* oocytes ruled out the first possibility. The correct targeting to the plasma membrane of *Xenopus* oocytes was traced by immunofluorescence microscopy. Oocytes expressing wild-type GLAST-1 and the chimeras G-M543 and G-N344 were strongly labeled along their perimeter by GLAST-1 antibodies and fluorescent second antibodies (Fig. 6 *A*, *2*, *3*, and *4*), consistent with the localization of the hybrid transporters at or close to the cell surface. Identical results were observed for all of the other chimeras with the fusion point between residue N344 and M543 (data not shown). In the case of water-injected control oocytes, no fluorescence was observed (Fig. 6 *A*, *1*). We conclude that the deletion of individual COOH-terminal sequences and/or the fusion of the reporter to the COOH terminus of full-length wild-type GLAST-1 (M543) or truncated GLAST-1 polypeptides abolish the glutamate transport properties of the expressed membrane-integrated glycoproteins. It should be noted that the point mutations in the transporter G-T382V/EL389FV, which was fully glycosylated at residue N380 and in G-EL389FV, which lacks the engineered *N*-glycosylation consensus site, also lead to a complete loss of the glutamate transport activity (data not shown). Both mutants are normally expressed (Fig. 4, lanes *9–12*) and correctly targeted to the plasma membrane (Fig. 6 *A*, *5* and *6*). In contrast, the functional properties of the mutated transporter G-T382V are comparable to wild-type GLAST-1 (data not shown) (Klöckner et al., 1993). This underlines the substantial influence of the amino acid substitution E389F combined with the exchange L389V on the activity of GLAST-1.

The NH_2 Terminus of GLAST-1 Is Exposed to the Cytosol

The orientation of the NH_2 terminus (EMR1 in Fig. 1 *B*) of GLAST-1 was examined by indirect immunofluorescence epitope mapping in a HEK cell line, permanently expressing wild-type GLAST-1 (HEK-GLAST) (Blau and Stoffel, 1995). If the first extramembrane region EMR1 is located in the cytoplasm, this domain should be accessible for a specific antibody only after permeabilization of the plasma membrane.

Affinity-purified antibodies raised against a synthetic peptide comprising residues 24–40 (P24–40) of GLAST-1 were generated. Only permeabilized HEK-GLAST cells were strongly labeled by immunofluorescence by these immunoglobulines (Fig. 6 *B*, *3* and *6*). Therefore the NH_2 terminus (EMR1) of GLAST-1 must be exposed to the cytosolic surface of the plasma membrane.

Fig. 6 *B* also visualizes the results of the control experiments. Intact HEK-GLAST cells were labeled with polyclonal rabbit anti-GLAST-1 antibodies (Storck et al., 1992), which also recognized extracellular transporter epitopes, and were impermeable for mAbs raised against α-tubulin. Permeabilization of cells with Triton X-100 was required to allow labeling with specific antisera against both α-tubulin and GLAST-1. Untransfected wild-type HEK cells showed no reaction with GLAST-1 antibodies (data not shown).

Discussion

We applied "reporter glycosylation scanning" to establish the complete topology of GLAST-1 in the plasma membrane. The localization of hydrophilic extramembrane regions was mapped to determine the number and orientation of membrane-spanning domains. We provide here experimental evidence for six presumably α-helical transmembrane domains in the NH_2-terminal part of GLAST-1, flanked by seven hydrophilic extramembrane regions. Fourfold glycosylated chimeras with a lumenal reporter indicated the inside–out orientation (cytosolic to extracellular) of TMD1, TMD3, and TMD5, and the twofold glycosylation of fusion proteins probed the reverse orientation of TMD2, TMD4, and TMD6. The specific fourfold glycosylation of chimeras G-P233 and G-Q313 proved that the reporter sequence placed at the COOH terminus of truncated GLAST-1 polypeptides is readily translocated across the ER membrane. The efficient *N*-glycosylation makes the

Published December 15, 1996

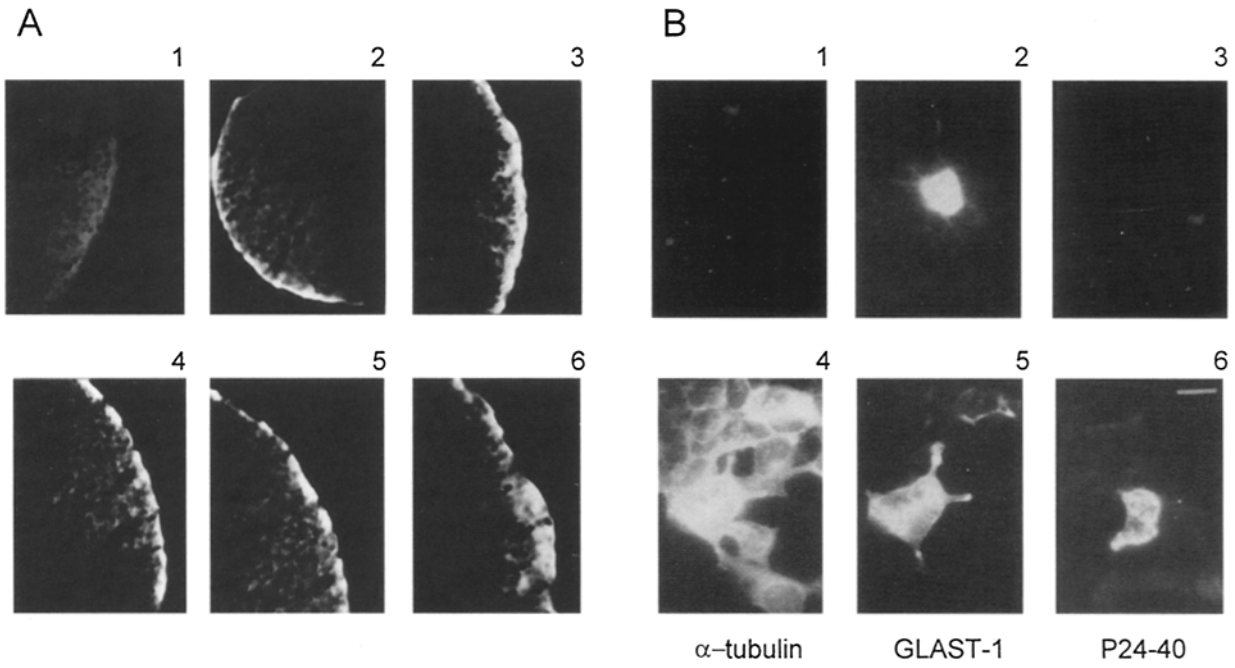

Figure 6. Wild-type, chimeric, and mutant GLAST-1 are located in the plasma membrane, and the NH_2 terminus of GLAST-1 resides in the cytoplasm. (*A*) Cryosections (15–20 μm) of *Xenopus* oocytes were incubated with anti–GLAST-1 antibody and stained with fluorescein isothiocyanate–conjugated second antibody. Wild-type GLAST-1 (*2*), G-M543 (*3*), G-N344 (*4*), G-EL389FV (*5*), and G-T382V/EL389FV (*6*) were expressed and targeted to the surface of oocytes with similar intensity. In the case of water-injected control oocytes (*1*), no fluorescence labeling was observed. (*B*) HEK 293 cells, permanently expressing wild-type GLAST-1, were immunostained with (*4–6*) and without (*1–3*) permeabilization of the plasma membrane (Triton X-100) as described under Materials and Methods. Cells were either doubly labeled with mouse monoclonal antitubulin and rabbit polyclonal anti–GLAST-1 antibodies (*1* and *2*, *4* and *5*) or labeled with rabbit polyclonal P24-40 antibodies (*3* and *6*). Second antibodies were fluorescein–anti-mouse IgG (*1* and *4*), fluorescein–anti-rabbit IgG (*3* and *6*) and cy3–anti-rabbit IgG (*2* and *5*). Staining of the cytosolic tubulin was only observed after disruption of membrane structures with Triton X-100 (*4*). Labeling of GLAST-1 at the cell surface was observed regardless of the integrity of the plasma membrane (*2* and *5*). The NH_2 terminus of GLAST-1 was labeled with P24-40 antibodies only after permeabilization of the plasma membrane (*6*), indicating its cytosolic orientation. Bar, 10 μm.

reporter sequence a reliable indicator of the extracellular or cytoplasmic sidedness of the tagged hydrophilic loops. Consistent with cell surface immunostaining of oocytes expressing G-N344 and G-M543, the reporter has no substantial influence on the folding of the transporter. Misfolded proteins would be retained in the biosynthetic compartments and then rapidly degraded. The signal for protein targeting from the ER via Golgi to the plasma membrane seems to be present within the NH_2-terminal 344–amino acid sequence. Immunostaining of HEK cells permanently expressing GLAST-1 gave evidence for the cytosolic localization of the NH_2 terminus (EMR1) of GLAST-1. This was expected from the absence of a cleavable signal sequence and from immunocytochemical labeling of astrocytes (Lehre et al., 1995). Phosphorylation of S113 by protein kinase C in GLT-1 (Casado et al., 1993) also agrees with intracellular localization of EMR3 connecting TMD2 and TMD3.

The extended, moderately hydrophobic COOH-terminal region of GLAST-1 is a feature uncommon for transporter proteins known so far. This domain is strongly conserved in the L-glutamate transporters GLAST-1, GLT-1, EAAC-1, and EAAT-4. The hydropathy plot exhibits at least seven short hydrophobic sequences 7–10 residues long (Fig. 1 *A*), implying that membrane-spanning segments in this region might be of shorter length. Our experiments with undeleted and deleted chimeras identified four of them as the core of the transmembrane domains TMD7–10, which are flanked by polar and charged residues. The topology of TMD8 could not be assigned with certainty by deleting residues F389–I397 in the fusion protein G-E406. Reporter inversion in the deletion mutant ΔG-E406 occurred only after in vitro translation but failed in the oocyte. We suggest that this might be due to an inherent topogenic activity keeping the tagged extramembrane region EMR9 on the cytoplasmic side of the ER membrane in the oocyte. The same observation was made for the deletion chimera ΔG-M543 with the reporter fused to the COOH terminus of wild-type GLAST-1. Positively charged residues, accumulating here in the tagged hydrophilic region EMR11, are known as a dominant topogenic determinant, which may prevent translocation of protein domains from the cytosol into the lumen of the ER (Boyd and Beckwith, 1989; von Heijne, 1989).

The shorter extension of TMD7 and TMD9 as compared to TMD1, TMD3, and TMD5 is likely to be reflected in the different glycosylation pattern of chimeras with the reporter sequence fused at the COOH terminus of inside–out-oriented transmembrane domains. The random distribution of bi- and tetra-antennary glycosylated fusion proteins, consistent with a random orientation of the COOH-terminal reporter to either side of the membrane, might be explained by the sequential insertion

Published December 15, 1996

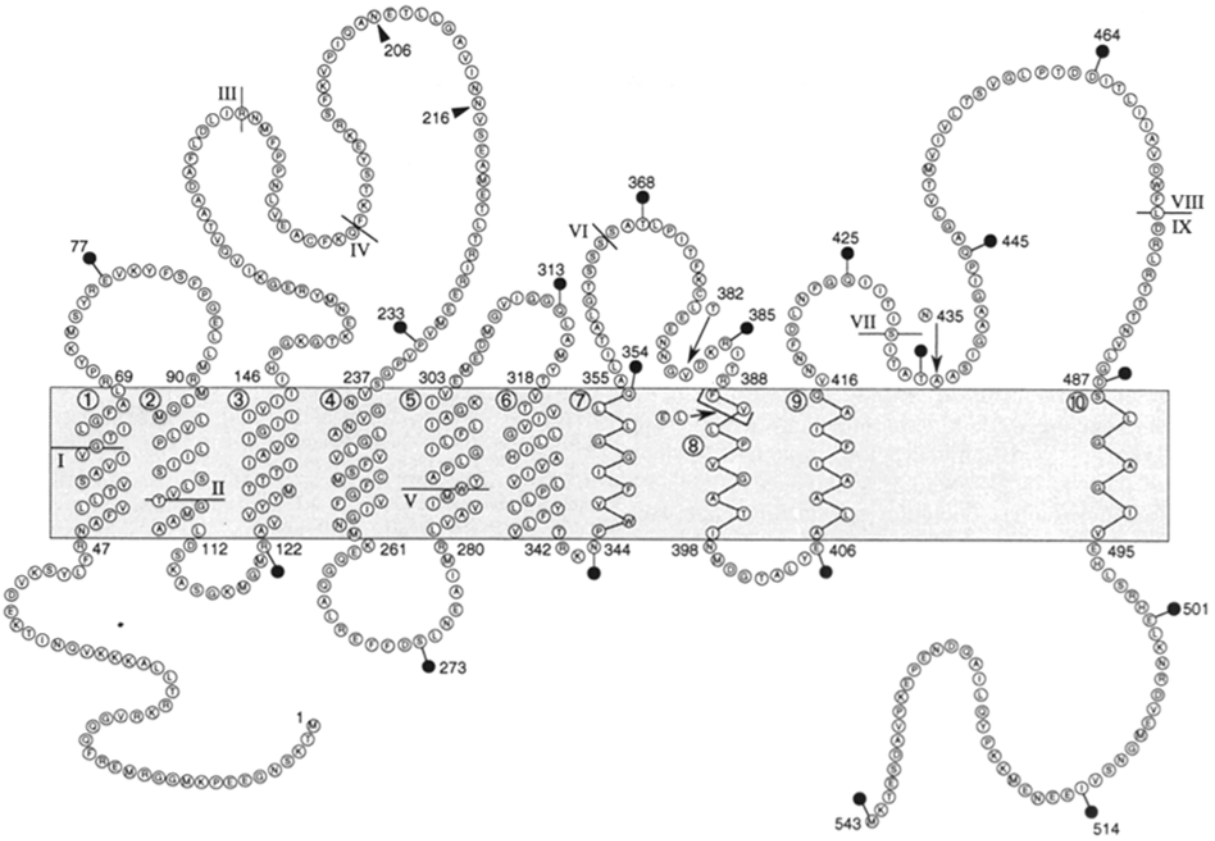

Figure 7. Proposed GLAST-1 topology in the plasma membrane. Native *N*-glycosylation sites are indicated by arrow heads. Filled circles mark the sites of GLAST-1, to which the reporter was fused, and arrows at residues 382 and 435 indicate the sites, that were mutated to obtain *N*-glycosylation mutants G-T382V, G-N435A, G-T382V/VSV, and G-T382V/EL389FV. The arrow at residues 389–390 points to the site where the 11-mer extension peptide was inserted. Exon boundaries are marked by roman numbers. Transmembrane domains, numbered TMDs 1–6, are likely to form α-helices, whereas TMDs 7–10 are considered to form β-sheets.

mechanism proposed for type IV membrane proteins like GLAST-1 (Blobel, 1980; Wessels and Spiess, 1988). In analogy to the translocation of secretory proteins and insertion of type II membrane proteins (Shaw et al., 1988), we suggest that during the last insertion cycle of chimeric GLAST-1 protein, the ultimate transmembrane domain acting as a signal anchor sequence and the translocating COOH-terminal portion of the growing polypeptide chain form a loop like structure in the proteinaceous (Görlich et al., 1992*a*, *b*; Mothes et al., 1994) and aqueous (Crowley et al., 1993, 1994) translocation channel (ER translocase) across the ER-membrane, with the attached reporter remaining in the cytoplasm. The interactions of the traversing signal anchor sequence with the proteins of the ER translocase and the degree of the lateral opening of the channel to the lipid core vary presumably with its length and hydrophobic properties (von Heijne, 1985, 1986; Nilsson et al., 1994; Martoglio et al., 1995). The efficient reporter glycosylation of chimeras G-E77, G-P233, and G-Q313 demonstrates that TMD1, TMD3, and TMD5, 20–23-hydrophobic residues-long, are firmly anchored in the lipid bilayer. After chain termination, the channel opening apparently remains wide enough to allow the reporter to translocate into the ER lumen. If the reporter is linked to TMD7 or TMD9, its random orientation toward the cytoplasmic or the lumenal surface of the ER membrane might be caused by two reasons. Membrane integration of the TMD partially fails because of a moderate hydrophobicity and therefore reduced interaction with the lipids, or membrane integration takes place but the narrow gated channel imposes a steric hindrance to the translocation of the COOH-terminal reporter into the lumen of the ER.

Since our experimental results combined with these considerations suggest shorter extensions of membrane spanning TMD7–TMD10 other than α-helical structures must be considered. β-Sheets require 7–10–amino acid residues to span the hydrophobic core of a membrane bilayer (Schirmer and Cowan, 1993). Intrabilayer β-sheet structures have been unequivocally demonstrated by x-ray analysis in porins (Cowan et al., 1992) and have also been proposed to occur in the acetylcholine receptor (Akabas et al., 1992), in the VDAC ion channel (Blachly-Dyson et al., 1990), and in lac permease (Radding, 1991). We propose β-sheet structures of the four COOH-terminal membrane-spanning regions of GLAST-1 but cannot rule out other conformations. Our experimental results and their interpretation fit best the membrane integration of GLAST-1 depicted in Fig. 7.

The topology profile proposed here facilitates the analysis of specific GLAST-1 domains or single–amino acid residues essential for neurotransmitter binding and translocation. Aromatic residues border the ends of transmem-

brane TMD7 (W346; F348), TMD8 (F389), and TMD9 (Y405; F412), similar to porins composed solely of a nonpolar surface of β-sheets buried in the lipid bilayer. Phenylalanine residues are oriented toward the lipid core whereas tyrosine hydroxy groups and tryptophan side chains point toward the lipid polar headgroups (Weiss et al., 1991; Cowan et al., 1992). The hydrophobic side chain of F389 of GLAST-1 is thought to be involved in the membrane anchorage of TMD8. Substitution of F389 by E389 combined with the conservative substitution L390V led to the GLAST-1 mutant transporters G-T382V/EL389FV and G-EL389FV, which have lost glutamate transport activity. The negative charge of E389 might shift the transmembrane segment TMD8 partially into an extracellular location. The distance between the membrane surface and the highly charged hydrophilic region surrounding residue N380 will thereby be enlarged and give access for the *N*-glycosylation machinery. This interpretation is consistent with the observation that N380 is only glycosylated in the triple mutant G-T382V/EL389FV, but not in the active single substitution mutant G-T382V carrying the intact transmembrane domain TMD8.

F389 is located in the most strongly conserved domain of the four cloned L-glutamate transporters, GLAST-1, GLT-1, EAAC-1, and EAAT-4. 29 out of 33 residues (amino acids 383–415) are identical. This sequence contains the transmembrane domains TMD8 and TMD9, which are joined by the short cytosolic loop EMR9. The adjacent side chains of Y405 and E406 in this EMR have recently been recognized to be essential for L-glutamate transport. In GLAST-1, the hydroxy group of Y405 is thought to interact with the γ-carboxylate group of the neurotransmitter glutamate passing through the channel (Conradt and Stoffel, 1995). For GLT-1, the corresponding E404 has been suggested to line the glutamate/aspartate permeation pathway (Pines et al., 1995). The deduced cytosolic localization of both residues (Fig. 7) excludes their direct participation in substrate binding but suggests an essential contribution to substrate translocation or dissociation on the inside of the plasma membrane. Furthermore, the close neighborhood of residues Y405 and E406 to TMD8 and TMD9 implies that both transmembrane segments might directly contribute to the formation of the translocation pore.

The topology model of GLAST-1 consisting of six membrane spanning α-helices and four shorter transmembrane domains presumably forming a β-sheet cluster is unique and defines a new class of transporter proteins. The assumption that clusters of transmembrane β-sheet structures are involved in the transport of neurotransmitter substrate will provide new dimensions for understanding the transport mechanism of the Na^+-coupled high affinity L-glutamate transporters. The highly conserved domain structure of all L-glutamate transporters isolated so far suggests that the 10-TMD model of GLAST-1, deciphered by these studies experimentally, might represent a novel membrane topology of transporter molecules common to the other L-glutamate transporters GLT-1, EAAC-1, and EAAT-4, and the neutral amino acid transporter ASCT-1.

This work was supported by the Deutsche Forschungsgemeinschaft, "Glutamattransporter, exzitatorische Synapse," Sto 32/34-1; SFB 243, "Molekulare Analyse der Entwicklung zellulärer Systeme," project A4; and the Fritz-Thyssen-Stiftung.

Received for publication 16 May 1996 and in revised form 12 October 1996.

References

Akabas, M.H., D.A. Stauffer, M. Xu, and A. Karlin. 1992. Acetylcholine receptor channel structure probed in cysteine-substitution mutants. *Science (Wash. DC).* 258:307–310.

Arriza, J.L., M.P. Kavanaugh, W.A. Fairman, Y.N. Wu, G.H. Murdoch, R.A. North, and S.G. Amara. 1993. Cloning and expression of a human neutral amino acid transporter with structural similarity to the glutamate transporter gene family. *J. Biol. Chem.* 268:15329–15332.

Blachly-Dyson, E., S. Peng, M. Colombini, and M. Forte. 1990. Selectivity changes in site-directed mutants of the VDAC ion channel: structural implications. *Science (Wash. DC).* 247:1233–1236.

Blakely, R.D., H.E. Berson, R. Fremeau, Jr., M.G. Caron, M.M. Peek, H.K. Prince, and C.C. Bradley. 1991. Cloning and expression of a functional serotonin transporter from rat brain. *Nature (Lond.).* 354:66–70.

Blau, R., and W. Stoffel. 1995. Rat and human glutamate transporter GLAST-1: stable heterologous expression, biochemical and functional characterization. *Biol. Chem. Hoppe-Seyler.* 376:511–514.

Blobel, G. 1980. Intracellular protein topogenesis. *Proc. Natl. Acad. Sci. USA.* 77:1496–1500.

Bouvier, M., M. Szatkowski, A. Amato, and D. Attwell. 1992. The glial cell glutamate uptake carrier countertransports pH-changing anions. *Nature (Lond.).* 360:471–474.

Boyd, D., and J. Beckwith. 1989. Positively charged amino acid residues can act as topogenic determinants in membrane proteins. *Proc. Natl. Acad. Sci. USA.* 86:9446–9450.

Casado, M., A. Bendahan, F. Zafra, N.C. Danbolt, C. Aragon, C. Gimenez, and B.I. Kanner. 1993. Phosphorylation and modulation of brain glutamate transporters by protein kinase C. *J. Biol. Chem.* 268:27313–27317.

Catty, D. 1988. Antibodies: A Practical Approach. IRL Press, Oxford. 121–137.

Colman, A. 1984. Translation of eukaryotic messenger RNA in Xenopus oocytes. *In* Transcription and Translation: A Practical Approach. B.D. Hames and S.J. Higgins, editors. IRL Press, Oxford. 271–302.

Conradt, M., and W. Stoffel. 1995. Functional analysis of the high affinity, Na^+-dependent glutamate transporter GLAST-1 by site-directed mutagenesis. *J. Biol. Chem.* 270:25207–25212.

Conradt, M., T. Storck, and W. Stoffel. 1995. Localization of N-glycosylation sites and functional role of the carbohydrate units of GLAST-1, a cloned rat brain L-glutamate/L-aspartate transporter. *Eur. J. Biochem.* 229:682–687.

Cowan, S.W., T. Schirmer, G. Rummel, M. Steiert, R. Ghosh, R.A. Pauptit, J.N. Jansonius, and J.P. Rosenbusch. 1992. Crystal structures explain functional properties of two *E. coli* porins. *Nature (Lond.).* 358:727–733.

Crowley, K.S., G.D. Reinhart, and A.E. Johnson. 1993. The signal sequence moves through a ribosomal tunnel into a noncytoplasmic aqueous environment at the ER membrane early in translocation. *Cell.* 73:1101–1115.

Crowley, K.S., S. Liao, V.E. Worrell, G.D. Reinhart, and A.E. Johnson. 1994. Secretory proteins move through the endoplasmic reticulum membrane via an aqueous, gated pore. *Cell.* 78:461–471.

Engelke, T., D. Jording, D. Kapp, and A. Puhler. 1989. Identification and sequence analysis of the Rhizobium meliloti dctA gene encoding the C4-dicarboxylate carrier. *J. Bacteriol.* 171:5551–5560.

Fairman, W.A., R.J. Vandenberg, J.L. Arriza, M.P. Kavanaugh, and S.G. Amara. 1995. An excitatory amino-acid transporter with properties of a ligand-gated chloride channel. *Nature (Lond.).* 375:599–603.

Flott, B., and W. Seifert. 1991. Characterization of glutamate uptake systems in astrocyte primary cultures from rat brain. *Glia.* 4:293–304.

Fremeau, R., M.G. Caron, and R.D. Blakely. 1992. Molecular cloning and expression of a high affinity L-proline transporter expressed in putative glutamatergic pathways of rat brain. *Neuron.* 8:915–926.

Fujiki, Y., A.L. Hubbard, S. Fowler, and P. Lazarow. 1982. Isolation of intracellular membranes by means of sodium carbonate treatment application to endoplasmic reticulum. *J. Cell Biol.* 93:97–102.

Goodfriend, T.L., L. Levine, and G. Fasman. 1964. Antibodies to bradykinin and angiotensin: a use of carbodiimide in immunology. *Science (Wash. DC).* 144:144–146.

Görlich, D., E. Hartmann, S. Prehn, and T.A. Rapoport. 1992*a*. A protein of the endoplasmic reticulum involved early in polypeptide translocation. *Nature (Lond.).* 357:47–52.

Görlich, D., S. Prehn, E. Hartmann, K.U. Kalies, and T.A. Rapoport. 1992*b*. A mammalian homolog of SEC61p and SECYp is associated with ribosomes and nascent polypeptides during translocation. *Cell.* 71:489–503.

Guastella, J., N. Nelson, H. Nelson, L. Czyzyk, S. Keynan, M.C. Miedel, N. Davidson, H.A. Lester, and B.I. Kanner. 1990. Cloning and expression of a rat brain GABA transporter. *Science (Wash. DC).* 249:1303–1306.

Hart, G.W., K. Brew, G.A. Grant, R.A. Bradshaw, and W.J. Lennarz. 1978. Primary structural requirements for the enzymatic formation of the N-glycosidic bond in glycoproteins. *J. Biol. Chem.* 254:9747–9753.

Hediger, M.A., M.J. Coady, T.S. Ikeda, and E.M. Wright. 1987. Expression

cloning and cDNA sequencing of the Na^+/glucose co-transporter. *Nature (Lond.).* 330:379–381.

Higuchi, R., B. Krummel, and R.K. Saiki. 1988. Recombinant PCR. A general method of in vitro preparation and specific mutagenesis of DNA fragments: study of protein and DNA interactions. *Nucleic Acids Res.* 16:7351–7361.

Kanai, Y., and M.A. Hediger. 1992. Primary structure and functional characterization of a high-affinity glutamate transporter. *Nature (Lond.).* 360:467–471.

Kanai, Y., S. Nussberger, M.F. Romero, W.F. Boron, S.C. Hebert, and M.A. Hediger. 1995. Electrogenic properties ot the epithelial and neuronal high affinity glutamate transporter. *J. Biol. Chem.* 270:16561–16568.

Klöckner, U., T. Storck, M. Conradt, and W. Stoffel. 1993. Electrogenic L-glutamate uptake in Xenopus laevis oocytes expressing a cloned rat brain L-glutamate/L-aspartate transporter (GLAST-1). *J. Biol. Chem.* 268:14594–14596.

Klöckner, U., T. Storck, M. Conradt, and W. Stoffel. 1994. Functional properties and substrate specificity of the cloned L-glutamate/L-aspartate transporter GLAST-1 from rat brain expressed in Xenopus oocytes. *J. Neurosci.* 14:5759–5765.

Kreis, T.E. 1986. Microinjected antibodies against the cytoplasmic domain of vesicular stomatitis virus glycoprotein block its transport to the cell surface. *Source.* 5:931–941.

Laemmli, U.K. 1970. Cleavage of structural proteins during the assembly of the head of bacteriophage T4. *Nature (Lond.).* 227:680–685.

Laskey, R.A., and A.D. Mills. 1975. Quantitative film detection of ^3H and ^{14}C in polyacrylamide gels by fluorography. *Eur. J. Biochem.* 56:335–341.

Lehre, K.P., L.M. Levy, O.P. Ottersen, J. Storm-Mathisen, and N.C. Danbolt. 1995. Differential expression of two glial glutamate transporters in the rat brain: quantitative and immunocytochemical observations. *J. Neurosci.* 15: 1835–1853.

Martoglio, B., M.W. Hofmann, J. Brunner, and B. Dobberstein. 1995. The protein-conducting channel in the membrane of the endoplasmic reticulum is open laterally toward the lipid bilayer. *Cell.* 81:207–214.

Mothes, W., S. Prehn, and T.A. Rapoport. 1994. Systematic probing of the environment of a translocating secretory protein during translocation through the ER membrane. *EMBO (Eur. Mol. Biol. Organ.) J.* 13:3973–3982.

Nilsson, I., P. Whitley, and G. von Heijne. 1994. The COOH-terminal ends of internal signal and signal-anchor sequences are positioned differently in the ER translocase. *J. Cell Biol.* 126:1127–1132.

Pacholczyk, T., R.D. Blakely, and S.G. Amara. 1991. Expression cloning of a cocaine- and antidepressant-sensitive human noradrenaline transporter. *Nature (Lond.).* 350:350–354.

Pines, G., N.C. Danbolt, M. Bjoras, Y. Zhang, A. Bendahan, L. Eide, H. Koepsell, J. Storm-Mathisen, E. Seeberg, and B.I. Kanner. 1992. Cloning and expression of a rat brain L-glutamate transporter. *Nature (Lond.).* 360:464–467.

Pines, G., Y. Zangh, and B.I. Kanner. 1995. Glutamate 404 is involved in the substrate discrimination of GLT-1, a (Na^+ + K^+)-coupled glutamate transporter from rat brain. *J. Biol. Chem.* 270:17093–17097.

Radding, W. 1991. Proposed partial β-structures for lac permease and the Na^+/H^+ antiporter which use similar transport and H^+ coupling mechanisms. *J. Theor. Biol.* 150:239–249.

Russel, M., and P. Model. 1982. Filamentous phage pre-coat is an integral membrane protein: analysis by a new method of membrane preparation. *Cell.* 28: 177–184.

Schirmer, T., and S.W. Cowan. 1993. Prediction of membrane-spanning β-strands and its application to maltoporin. *Protein Sci.* 2:1361–1363.

Schulte, S., and W. Stoffel. 1995. UDP-galactose: ceramide galactosyltransferase and glutamate/aspartate transporter. Copurification, separation and characterization of the two glycoproteins. *Eur. J. Biochem.* 233:947–953.

Shafqat, S., B.K. Tamarappoo, M.S. Kilberg, R.S. Puranam, J.O. McNamara, A. Guadano-Ferraz, and R. Fremeau. 1993. Cloning and expression of a novel Na^+-dependent neutral amino acid transporter structurally related to mammalian Na^+/glutamate cotransporters. *J. Biol. Chem.* 268:15351–15355.

Shaw, A.S., P.J.M. Rottier, and J.K. Rose. 1988. Evidence for the loop model of signal sequence insertion into endoplasmic reticulum. *Proc. Natl. Acad. Sci. USA.* 85:7592–7596.

Shimada, S., S. Kitayama, C.L. Lin, A. Patel, E. Nanthakumar, P. Gregor, M. Kuhar, and G. Uhl. 1991. Cloning and expression of a cocaine-sensitive dopamine transporter complementary DNA. *Science (Wash. DC).* 254:576–578.

Singh, P., B.L. Tang, S.H. Wong, and W. Hong. 1993. Transmembrane topology of the mammalian KDEL receptor. *Mol. Cell. Biol.* 13:6435–6441.

Smith, K.E., L.A. Borden, P.R. Hartig, T. Branchek, and R.L. Weinshank. 1992. Cloning and expression of a glycine transporter reveal colocalization with NMDA receptors. *Neuron.* 8:927–935.

Storck, T., S. Schulte, K. Hofmann, and W. Stoffel. 1992. Structure, expression, and functional analysis of a Na^+-dependent glutamate/aspartate transporter from rat brain. *Proc. Natl. Acad. Sci. USA.* 89:10955–10959.

Tolner, B., B. Poolman, and W.N. Konings. 1992*a*. Characterization and functional expression in Escherichia coli of the sodium/proton/glutamate symport proteins of Bacillus stearothermophilus and Bacillus caldotenax. *Mol. Microbiol.* 6:2845–2856.

Tolner, B., B. Poolman, B. Wallace, and W.N. Konings 1992*b*. Revised nucleotide sequence of the gltP gene, which encodes the proton-glutamate-aspartate transport protein of Escherichia coli K-12. *J. Bacteriol.* 174:2391–2393.

Uhl, G.R. 1992. Neurotransmitter transporters (plus): a promising new gene family. *Trends Neurosci.* 15:265–268.

von Heijne, G. 1985. Signal sequences. The limits of variation. *J. Mol. Biol.* 184: 99–105.

von Heijne, G. 1986. Towards a comparative anatomy of N-terminal topogenic protein sequences. *J. Mol. Biol.* 189:239–242.

von Heijne, G. 1989. Control of topology and mode of assembly of a polytopic membrane protein by positively charged residues. *Nature (Lond.).* 341:456–458.

Weiss, M.S., U. Abele, J. Weckesser, W. Welte, E. Schiltz, and G.E. Schulz. 1991. Molecular architecture and electrostatic properties of a bacterial porin. *Science (Wash. DC).* 254:1627–1630.

Wessels, H.P., and M. Spiess. 1988. Insertion of a multispanning membrane protein occurs sequentially and requires only one signal sequence. *Cell.* 55: 61–70.